Use of X-ray CCDs in the calibration of the flight mirrors for the JET-X telescope on Spectrum-X

C.M.Castelli[1], H.Braüninger[2], W. Burket[2], S.Campano[3], G.Cusumano[4], M. Denby[1], R.Egger[2], N.Nelms[1], M.R.Sims[1], D.J.Watson[1], A.Wells[1] and R.Willingale[1]

1 X-ray Astronomy Group, Department of Physics and Astronomy, University of Leicester, Leicester, LE1 7RH, UK

2 Max-Plank Institute fur Extraterrestriche Physik, Gautingerstr. 45, D-82061, Neurid, Germany

3 Osservatorio di Brera, Via E. Bianchi 46, I-22055 Merate, Italy

4 CNR, Instituto di Fisica Cosmica, Via M.Stabile, 172-90139 Palermo, Italy

ABSTRACT

The X-ray mirror calibration programme for the JET-X telescope on Spectrum-X has recently been carried out at the 130m long Panter X-ray beam line of the Max Plank Institute fur Extraterrestriche Physik. The excellent spatial resolution achieved with these mirrors, 15 arcsec half energy width (HEW) at 1.5keV and 19 arcseconds at 8keV, has proved to be difficult to measure precisely using previously established calibration methods (involving either slit detectors or the ROSAT PSPC imaging proportional counter). New diagnostic techniques have, therefore, been developed using a CCD imaging camera which utilised newly available X-ray CCD technology.

Details of the calibration technique and the performance of the camera are provided and results are compared with those obtained from the slit and PSPC detectors.

1.INTRODUCTION

The Joint European X-ray Telescope (JET-X) is one of four core instruments on the Spectrum-X astrophysics mission aimed at studying high energy astrophysical sources in the X and γ-ray energy bands. The primary science objective of JET-X is to carry out high resolution X-ray measurements of cosmological sources (e.g. quasars and AGN) with high angular efficiency and spectroscopic resolution[1]. The spacecraft is due for launch in December 1997 into a highly elliptical orbit with a period of four days.

JET-X consists of two identical, co-aligned telescopes employing grazing incidence Wolter-I type mirrors each possessing a spatial resolution of better than 20 arcsec half energy width throughout the 0.3 to 10keV energy band. The focal length of the mirrors is 3500mm with a combined total effective area of 330cm^2 at 1.5 keV, falling to 145cm^2 at 8keV. The focal plane imaging detectors for each telescope comprise an assembly of two, cooled X-ray sensitive CCDs, providing an area coverage of 20 arcminutes diameter. These detectors have been developed specifically to provided high spatial (27μm pixel) and energy resolution (130eV at 6keV) with good detection efficiency in the telescope energy band[2].

To ensure that in the final flight mirror assemblies, the JET-X mirror performance specification could be achieved, the manufacturing process and integration of the mirror shells was validated using an Engineering Qualification Mirror (EQM) module. The EQM was flight-like in its design and construction except that it contained only 10 active shells of flight quality. The remaining 2 shells were blanked off since they failed to show the necessary full width at half maximum intensity (FWHM) during individual UV testing of the shells prior to integration. The inclusion of these shells would have resulted in an not representative imaging performance for the final mirror assembly.

Calibration of the X-ray performance was carried out at the X-ray long-beam Panter calibration facility of the Max Plank Institute fur Extraterrestriche Physic in Munich. Both prior to and following flight level vibration qualification tests, the imaging performance was assessed using the ROSAT position sensitive proportional counter (PSPC) and slit detector that were available at the Panter facility. A resolution of 30 arcseconds was

0-8194-2196-0/96/$6.00

measured with the EQM, but this measurement proved to be difficult using the PSPC because of its low, intrinsic resolution (120 arcseconds) and poor sensitivity above 3keV. A different approach was therefore adopted for the flight mirrors, in order to provide better detector resolution. A CCD camera system with high spatial resolution and detection efficiency was commissioned for the FM mirror programme making use of newly available CCD technology developed for the EPIC CCD camera on XMM[3].

The X-ray mirror calibration programme for the FM mirror modules has recently been concluded. Details of the CCD camera and the diagnostic techniques employed in the FM calibration are described in this paper. Results are summarised and comparison with the PSPC measurements are also made.

2.THE PANTER FACILITY AND PSPC DETECTOR

The Panter test facility is purpose-built to support development and calibration of instrumentation for space borne X-ray astronomy[4]. It comprises an X-ray source, connected to a large instrumentation tank via a 130m long beam line which is continuously maintained under a high vacuum typically around 10^{-6} mBar. The instrumentation tank has a circular diameter of 7m and a length of 12m and can accommodate complete X-ray telescope. The telescope can be mounted on a table for positioning and a series of manipulators allows movement of the X-ray calibration detectors and other support instrumentation. The tank opens into a class 1000 clean-room to maintain cleanliness of the instruments during installation into the tank.

Two X-ray sources are used to cover the soft X-ray (0.2 - 5keV) and hard X-ray (5-20keV) energy ranges. These sources can operate with maximum count rates of up to 50,000 counts/sec/cm2 at the tank end. The whole beam line is maintained under an oil free vacuum by a series of turbomolecular pumps with catalysor traps and cryopumps to reduce the partial pressure of water.

X-ray calibration of the telescope subsystems are carried out using the ROSAT engineering model imaging PSPC[5]. This is a multiwire proportional counter with a cathode strip readout scheme for position determination. The front entrance window is 8cm in diameter and is made of thin (1um) polypropylene coated with carbon to reduce UV transmission. The window is supported by a thin mesh with 72% transmission. The spatial resolution depends on X-ray energy and is around 120 μm HEW at 1keV. The quantum efficiency falls rapidly below 3 keV from 63% to a value of around 10% at 500eV due to the decreasing window transmission. At higher energies, the efficiency is limited to the absorption in the gas which limits the efficiency to around 40% at 8kev. The energy resolution of the PSPC approaches that for a single wire proportional counter and obeys the relationship

$$\Delta E(\mathrm{FWHM}) = 0.41 E(\mathrm{keV})^{1/2}$$

over the entire sensitive area of the counter. The dead time of the counter has been measured to be in the range 180 to 280 μs and typically the maximum count rate to avoid significant counter dead time is around 1000 to 2000 counts/second.

3.DESCRIPTION OF THE X-RAY CCD CAMERA

The CCD camera for the FM mirror calibration was designed and built at Leicester University and employs a CCD sensor of the type that is currently being developed for the EPIC camera on XMM[6]. The device is fabricated on 65 μm thick epitaxial silicon that has a high resistivity, in excess of 4000 Ωcm. This high resistivity enables the epitaxial layer to be depleted down to a depth of around 40 μm, thus extending the high energy detection efficiency. Secondly, the sensor utilises an 'open electrode' structure on the front surface to enhance the low energy efficiency by minimising the absorption in the overlying structure. The efficiency is further enhanced by extending the area occupied by the thin electrode area relative to the other electrodes, to cover 60% of the total available pixel area and further gains are made by etching a hole into the thin electrode down to the gate dielectric. To control the surface potential in the vicinity of the hole, a shallow p+ implant is located under the open region. This pins the local surface potential to the substrate level with efficient charge transfer maintained through the use of the three phase electrode structure. The resulting dead layer for the open electrode is around 850A and QEs in excess of 90% has been measured for this device at 1.5keV.

The CCD is cooled to its operating temperature of -80C to minimise dark current. Cooling is provided by liquid nitrogen which is fed into the main tank using copper feed pipes which are attached to a CCD cold finger block. Mounted next to the CCD camera head is the first stage preamplifier board. A single shielded ribbon cable carries the clock and bias voltages to the CCD. The CCD drive electronics and analogue processor are located outside the vacuum tank. This is a CAMAC based system, controlled by a RISC PC which also handles CCD data acquisition via a 12-bit ADC and dual slope integrator (CDS processor). The CCD bias voltages are provided by buffered, software programmable DACs, while the CCD clock sequences and CDS processor timing signals are generated by a programmable module based around a DSP chip, which provides flexible, parameter driven operation. The sequencer clock outputs are translated to the programmable CCD clock voltage levels by a driver board using hybrid circuits which also produce the correct waveform edges for the CCD. Dedicated software enables spectral analysis of the image data and control of the camera system. An electronics block diagram for the camera system is shown in Figure 1.

The CCD is operated in a frame store mode with an imaging area of 820 × 512 pixels (pixel size 27 μm square), giving a total active area of almost $3cm^2$. The camera has two gain settings depending on the type of measurement being carried out. In the high gain mode, the CCD photon counts and the system gain of 4eV/ADC produces a system noise level of less than 6 electrons rms at a pixel readout rate of 200kHz. This mode is used for measurements of mirror effective area because the energy resolution of the CCD enables photon fluxes of a particular line energy to be measured. In the low gain mode, the system gain is reduced to around 40eV/ADC. This increases the dynamic range of the analogue processor so that the CCD can be operated efficiently as an integrating detector rather than for photon counting. For example, at 8keV, the count rate in any single pixel can be as high as 20 photons per frame, thus increasing the throughput of the system and reducing the acquisition time for the X-ray images. However, there is no spectral information available from this data and so this mode is only useful for imaging provided that the source is mono-energetic and free from secondary X-ray lines and continuum. The CCD images are analysed off line using the 'Q' image analysis software developed at Leicester University[7]. The software can process the raw CCD data files into FITS file formats and perform all the necessary image and pulse height spectral analysis for the tests. Each frame of data from the camera is directly sent to a UNIX workstation running the Q software, allowing rapid image processing in parallel with the data collection. Finally, in front of the CCD is a thin aluminium/lexan filter supported on a 75% transmissive mesh. This filter blocks out optical photons from the source which would be a source of additional noise in the CCD.

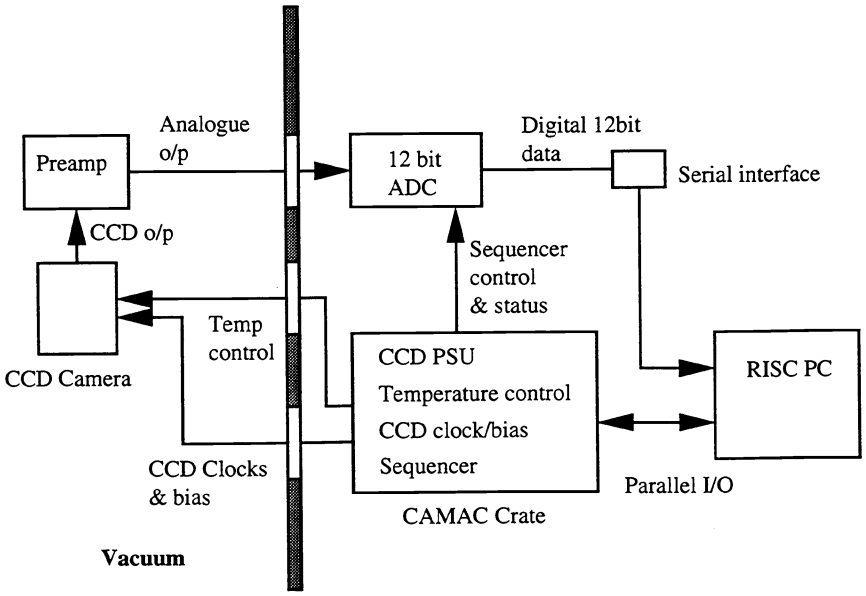

Figure 1 Schematic diagram of the CCD camera electronics

4. THE FLIGHT MODEL MIRRORS

The JET-X flight mirrors comprise a set of 12 mirror shells per module fabricated by a nickel electroforming replication processes that was developed for the SAX programme[8]. The nickel mirrors were replicated at the Medialario company from a set of 12 precision mandrels manufactured by Carl Ziess, Germany. After replication each mirror shell was tested using UV light on the optical bench at the Brera Observatory to obtain an initial estimate, from the optical point spread function, of whether the mirror figure was within the design limits. HEW measurements for individual flight mirror shells from these tests were found to lie in the range 7 and 12 arcseconds. X-ray tests are required to determine the contributions due to micro-roughness and the accuracy to which the 12 mirror shells can be assembled into the mirror mounting structure.

5. THE FLIGHT MIRROR CALIBRATION PROGRAMME

The primary aim of the mirror calibration is to verify all the mirror performance parameters at two energies, 1.5keV and 8.05 keV, of the X-ray energy response range. Additional measurements were taken at other intermediate energies. Results from this calibration, combined with mirror EXAFS, reflectivity measurements[9] and theoretical ray tracing are then used to determine the complete mirror response function.
The calibration programme therefore consists of the following measurements at each energy

- Determination of the focal length
- On and off-axis point spread function and vignetting function
- Geometric mirror distortions and gravity effects
- Effective area
- Continuum edge measurements
- Comparison of PSPC and CCD measurements of effective area

These measurements and the results are discussed in detail in the following sections.

5.1 Measurement of the mirror focal length

The best measure of the mirror resolution is through the encircled energy values. Values of FWHM are insensitive to extended wings in the mirror point spread function caused by scatter of the X-ray beam. This is mainly due to mirror surface micro roughness and is particularly noticeable at higher energies. The half energy width was, therefore, used to determine the optimum focus of the telescope mirrors can be determined.

Mirror focal length was determined by measuring the change in the mirror HEW as a function of focal distance for X-ray energies of 1.5 and 8keV. Figure 2a shows the data obtained with the CCD camera. These measurements, combined with curve fitting to the data, enable the mirror focal length to be determined to within 0.2mm. At this position the HEW across the energy band is less than 20 arcseconds and well within the overall mirror specification of 30 arcseconds. These curves also confirm the prediction from ray tracing that the focal point does not vary with X-ray energy and that the mirror HEW is very sensitive to the detector position. Thus, in order to preserve optimum mirror resolution, the JET-X focal plane CCD detector needs to be positioned to within ±0.5 mm of the focus. This error margin ensures that the loss of resolution is less than a few percent. At significantly larger distances the degradation is more severe. For example at a detector distance of ±7mm from the focus, the HEW is reduced by a factor of two.

The focal length is measured by positioning the CCD at the optimum focus and then measuring the distance between a fixed reference point on the mirror assembly and measurement blocks on either side of the CCD. This is done using a carbon fibre rod with micrometer attachment which allows the focal length to be measured to an overall accuracy of better than 0.5 mm.

Figure 2b shows the equivalent variation in HEW of the mirror to detector distance for the FM1 mirror assembly but this time using the PSPC detector. The observed optimum focal position is now dependent on energy and varies by around 6mm between 1.5 and 8keV. The reason for this variation is due to the change in absorption length of the X-rays in the gas with X-ray energy. Between 1 and 6 keV, the absorption path length differs by around 40 mm so that there is no precise fixed focal point within the detector gas volume with

energy. This leads, therefore, to a corresponding uncertainty in the measured focal position. In the case of the CCD detector, this effect is negligible since the X-ray interactions occur primarily in the narrow (<100μm) epitaxial layer of the device and the optimum focal position can thus be precisely located.

It follows that, PSPC measurements of the focal length are suitable for determining the optimum focal position with sufficient accuracy to preserve the intrinsic mirror resolution. Reliance upon PSPC measurements alone would result in an error of up to 3 mm in the focal length, which could result in a degradation in the mirror HEW by as much as 35%. The CCD therefore provides a far better means of determining the optimum telescope focus.

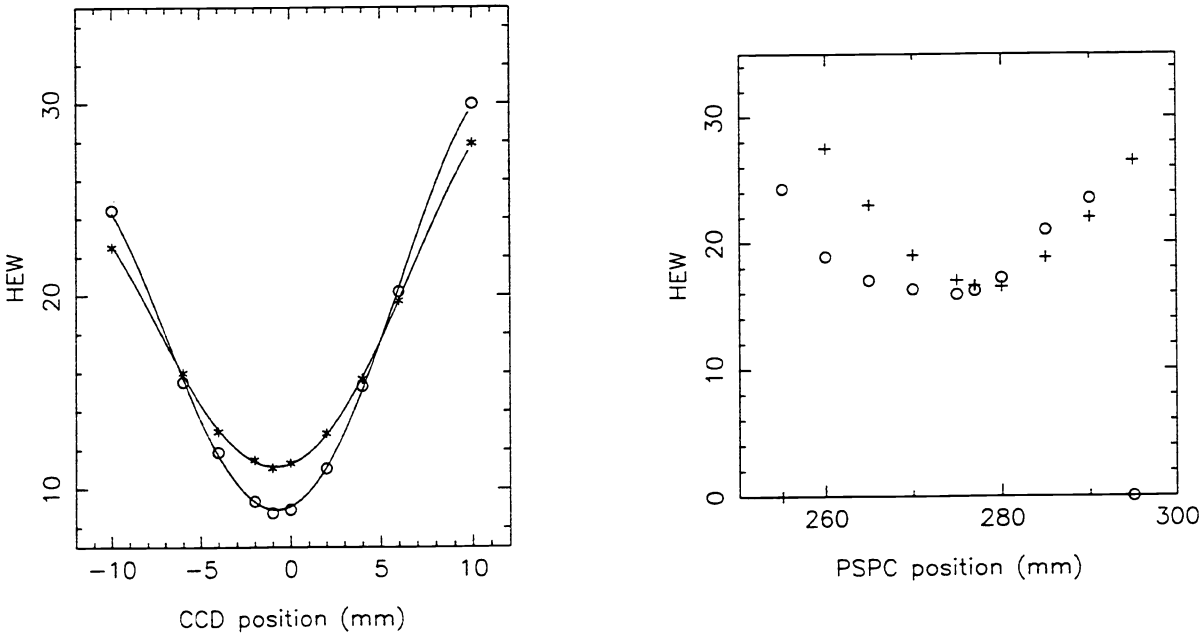

Figure 2 Mirror focal length measurements with the CCD (a) and PSPC (b)

5.2 Measurement of the point spread function

Figures 3 and 4 show deep X-ray exposures at 1.5keV and 8keV respectively, obtained with the CCD at the optimum mirror focal position. The plots are shown on a logarithmic scale to enhance any low level scatter wings. The image was acquired in 10 minutes and is made up of around 3×10^5 X-ray events. The CCD images are able to clearly reveal fine detail structure in and around the central core of the focused spot. The dark radial pattern visible is due to shadowing caused by the obscuration of the mirror spider and the bright radial lobes inbetween are a result of mechanical distortion of the mirror shells at the spider mounting points. Figure 5a & b show corresponding images obtained with the PSPC detector. Comparison with the CCD images shows that much image definition has been lost as a result of the lower PSPC spatial resolution. In order to estimate the mirror point spread function using the PSPC a correction factor needs to be applied to account for the finite response of the detector. It is assumed that the overall mirror response is given by the quadrature summation of the gaussian distributions that define the mirror and PSPC resolutions respectively. This assumption, however, is only valid if the point spread function of the PSPC is small compared to that of the mirror. In practice, this is found only to be the case for low X-ray energies where the absorbing power of the gas is higher. Thus, good agreement is found for the mirror HEW at 1.5 keV obtained using the two cameras, whereas at 8keV, the values are found to differ by up to 6%.

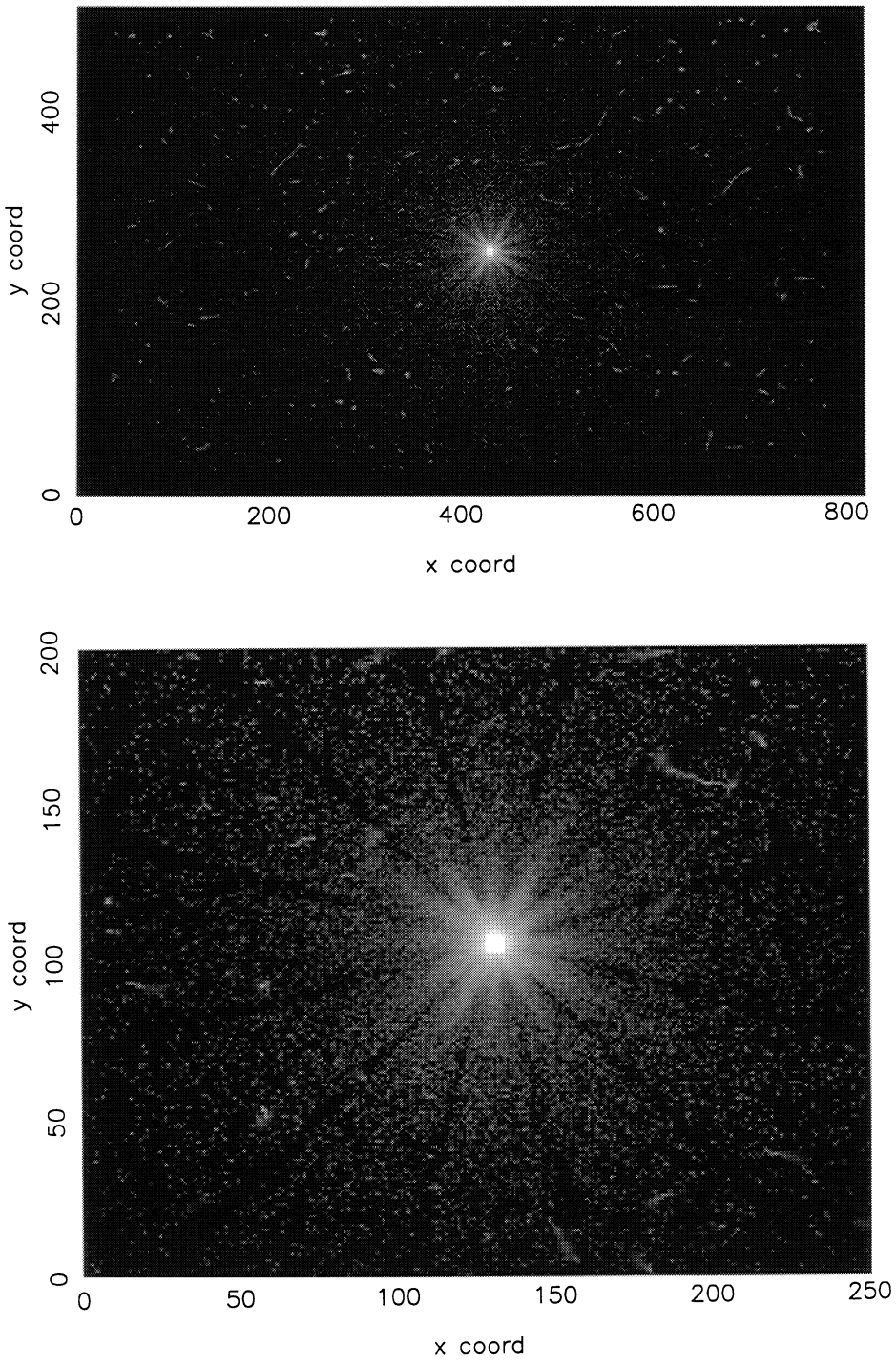

Figure 3 Deep X-ray exposure at 1.5 keV obtained with the CCD at the optimum mirror focal position. Top image shows the full CCD area and the bottom image is a magnified view of the region around the central core.

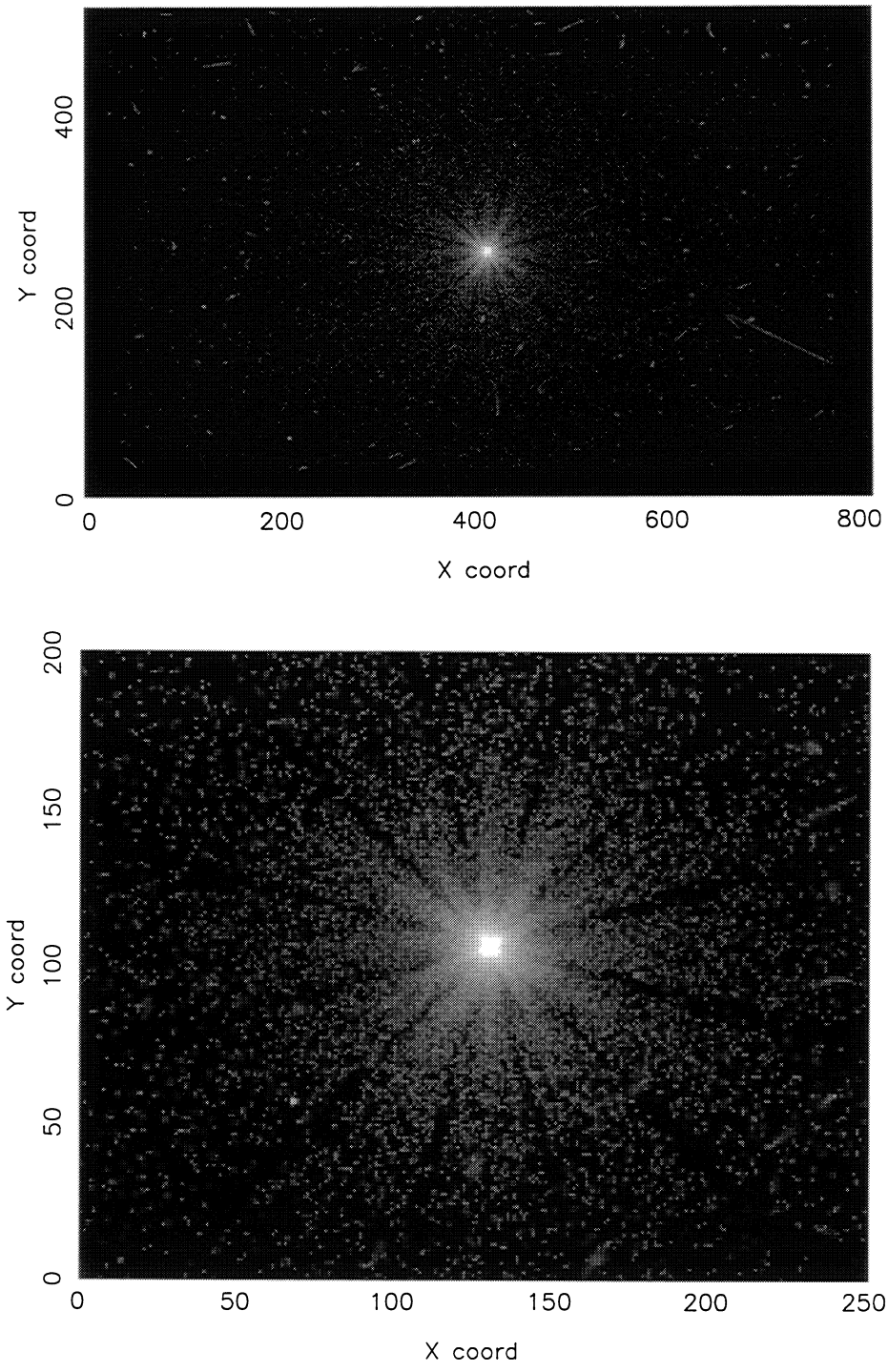

Figure 4 Deep X-ray exposure at 8.05 keV obtained with the CCD at the optimum mirror focal position. Top image shows the full CCD area and the bottom image is a magnified view of the region around the central core.

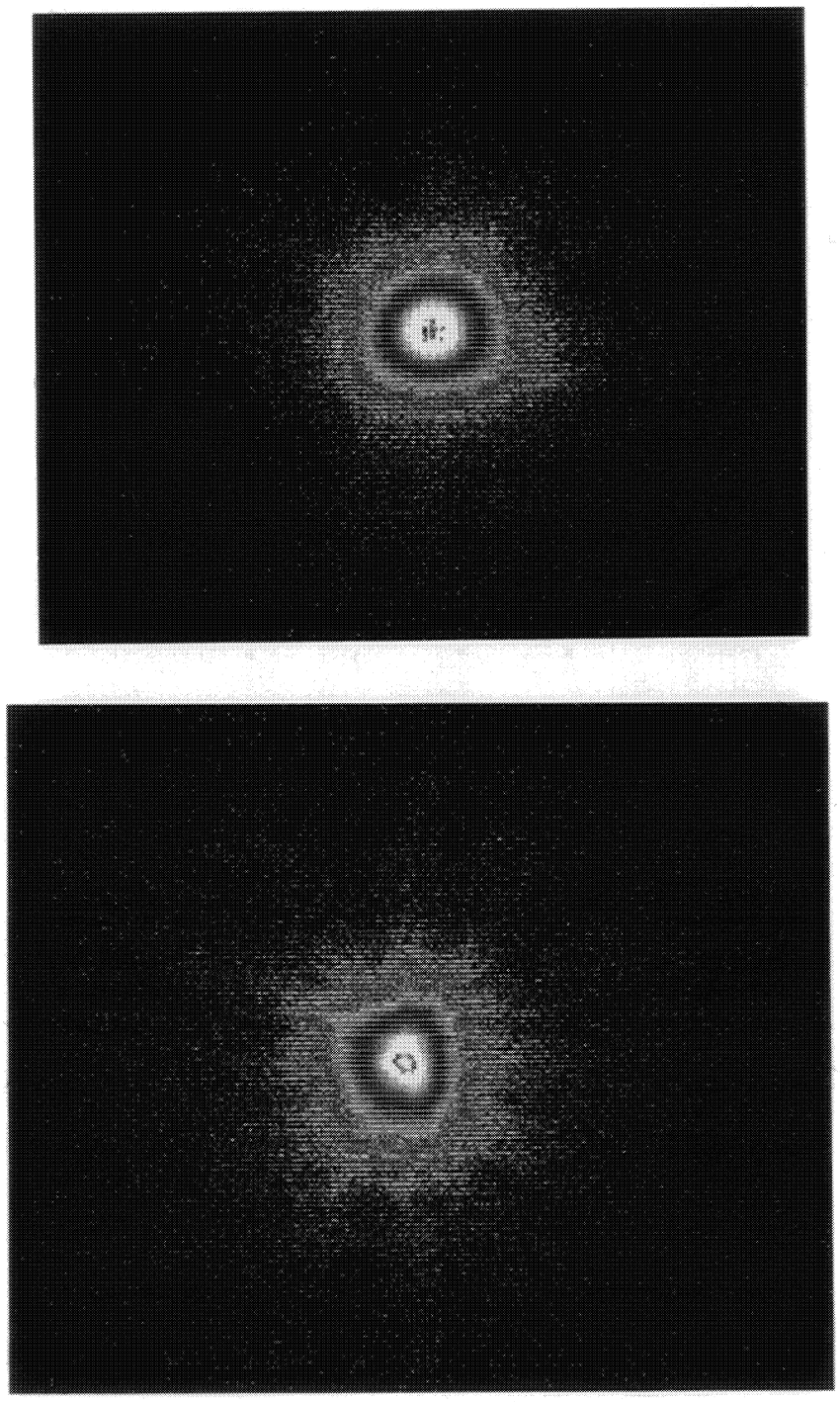

Figure 5 PSPC images at the optimum mirror focal length for X-ray energies of 1.5 keV (top) and 8keV (bottom)

Prior to the use of the CCD detector, a slit detector with a 0.1mm slit was used to try to make higher spatial resolution measurements of the mirror response. Scan measurements with this detector give a better estimate of the HEW, however, this technique suffers from the disadvantage that it can only provide the line spread function for a single axis and information about mirror asymmetry and other image details are therefore lost.

The CCD resolution is sufficiently high to allow a direct measurement of the ability of the mirror to resolve the images of two identical point sources separated by a known angular separation. A separation of 20 arcseconds was chosen to reflect the scientific specification for JET-X and the two sources were simulated by moving the CCD laterally by a distance equivalent to 20 arcseconds in the focal plane half way through the image exposure. Figure 6(a) shows a 3D plot of the intensity distributions for the two point sources at 1.5keV and shows that they can be easily resolved by the optics. A line scan through the distributions (b) shows that the overlap point occurs at around 25% of the peak intensity; within the half-intensity criterion for the minimum resolution of two point sources (Rayleigh Criterion). At 8keV, the effect of scatter is more pronounced and the overlap point increases to around 35% of the peak, but is still sufficiently small to achieve the resolution criterion.

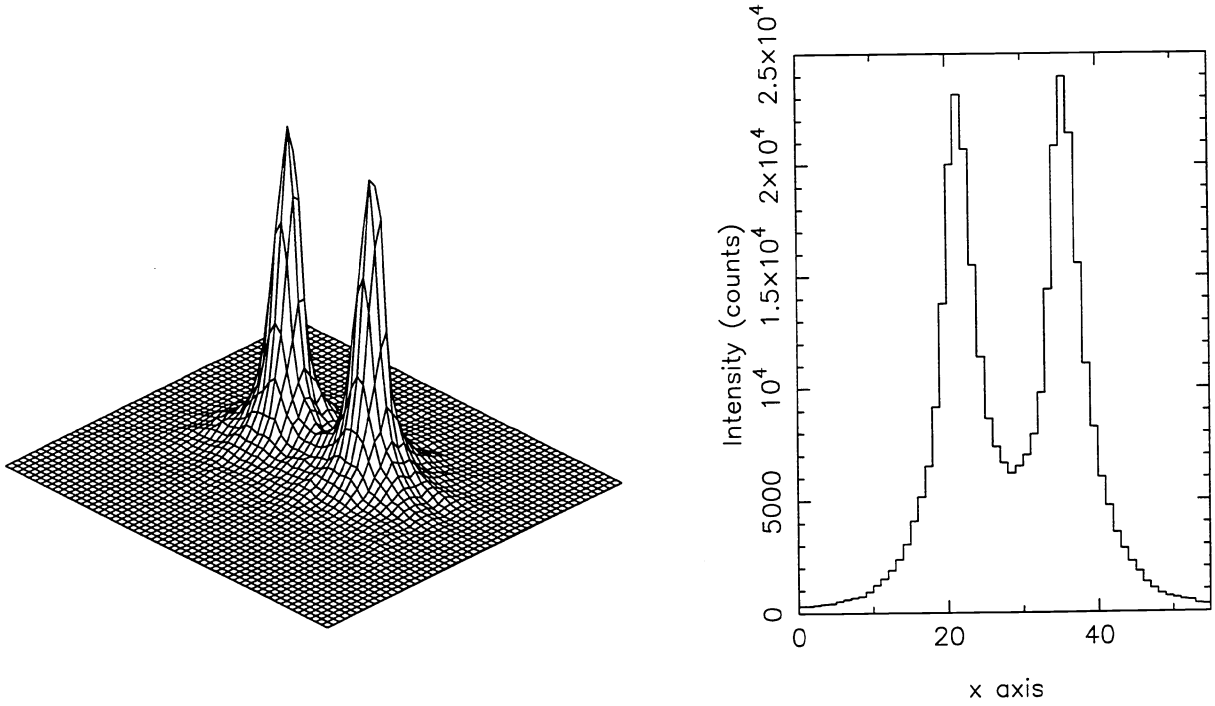

Figure 6 A 3D plot showing the ability of the JET-X mirrors to resolve 2 point sources separated by 20 arcsec(a). A line scan through the same plot (b) showing the cross over intensity level.

A disadvantage of this CCD camera is that its active area is not large enough to cover the full field of view of the X-ray mirrors. This is a shortcoming at high energies where there is a significant flux component scattered out to large angles, and, at 8keV the wings in the mirror point spread function extend well beyond the CCD image area. Consequently, the CCD underestimates the encircled energy fraction. Thus, to calculate these values and determine the mirror micro-roughness from the scatter profile, the PSPC counter has to be used. An alternative approach, of extrapolating the CCD scatter profiles using a first order approximation to the measured data, is considered to be subject to unacceptable error.

Finally, investigations of mirror geometric distortions have been carried out by placing the CCD in an out-of-focus position 100mm in front or behind the optimum focus. In these positions, the detector intercepts the light cone of the optics, thus forming a large annular image that enables any image asymmetry to be readily observe. Figure 7(a) shows the image produced for FM1 at 1.5 keV on a logarithmic scale. The annular image has a diameter of around 300 pixels and shows the sharp radial pattern due to the spider obstruction and the lobe-like structure around the annulus caused by the mirror mounting points. The quasi-rectangular grid

superimposed on the image is due to the support grid of the CCD light filter. The central bright region is due to the integral effect of the scattering wings in the point spread function from the annular elements of the mirror. Figure 7(bottom) shows a 3D projection of the annular intensity distribution which shows the relative intensity of these features at 1.5 keV. Little asymmetry is observed in these images showing that the shells have been assembled with good concentricity. By comparison, a PSPC image shown in Figure 8 for the same intra-focal position, shows less image detail.

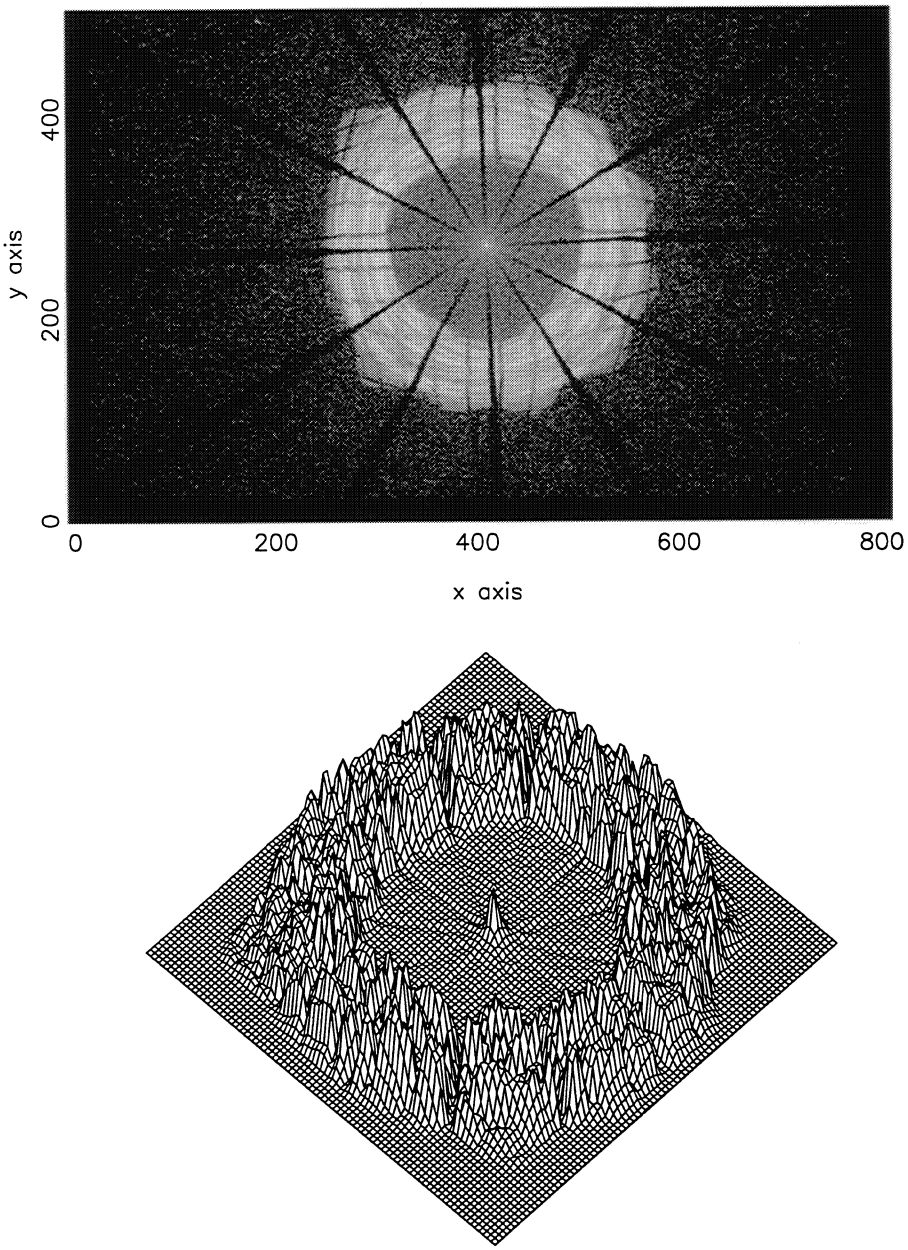

Figure 7 Out-of focus image at 1.5 keV obtained with the CCD revealing little geometric distortion by the mirror (top). A 3D plot of the same image (bottom)

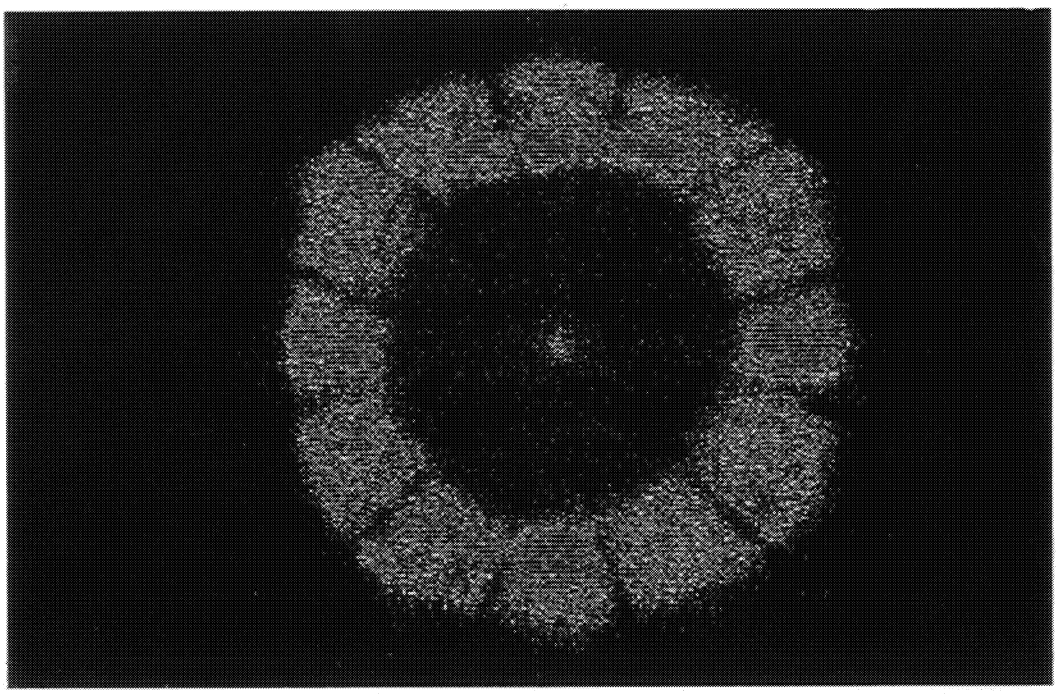

Figure 8 PSPC image at the mirror intra-focal position

5.3 Mirror Effective Area

Mirror collecting area has been measured using both the PSPC and CCD detectors by comparing the ratio of the mean X-ray count rate (photons/sec), focused by the optics, to the incident, flat field count rate (photons/sec/cm2). This measurement requires translation of the mirror assembly in and out of the detector field of view. Although in principle measurement of the effective area is straight-forward, in practice, it is difficult to achieve the required accuracy using the CCD detector. The main reason for this arises as a direct consequence of the large collecting area of the mirrors.

For a given count rate observed at the mirror focus, I_{foc}, the corresponding number of counts detected per frame in the flat field, N_{flat}, is given by the expression

$$N_{flat} = I_{foc} \times \frac{A_{ccd}}{A_{eff}}$$

where A_{ccd} is the CCD area and Aeff is the mirror effective area. Since the ratio of mirror to CCD area can be as high 50 to 60, the corresponding flat field exposure time required to achieve a comparable counting error would be of the order 1.5×10^4 seconds. This is clearly impractical. The detector throughput can, however, be increased by defocused the X-ray image. By placing the defocus position at 80mm to produce an annular image on the CCD without significant loss of counts outside the detector imaging area, a significantly higher flux from the optics can be tolerated before the X-ray spectra starts to show evidence of pulse pile-up. Even so, the measurement period to achieve a 1% counting error from the flat field rate still remains in excess of 10 hours. A

compromise therefore has to be made between the time to carry out the measurement and the final error due to the counting statistics. An error value for the measurement of around 3% (1000 counts) has been achieved in these measurements reported here.

Another source of error is due to instabilities in the source output flux over the long integration time. If this is not corrected for then a significant systematic error is introduced into the measurement. To correct for source variations, the count rate has been monitored using a counter placed in the direct beam but out of the field of view of both the optics and imaging detector. Although this enabled large variations in source output, typically around 10% over several hours, to be corrected, a 1-2% error remains in the correction factor from the monitor counter. This is due to the limited number of counts detected as a result of its small area and detection efficiency. Thus the overall precision for the mirror effective areas using the CCD detector, given by the quadrature summation of all the error sources, is around 5 to 6%.

The PSPC has a much larger area and higher count rate capability. Effective area measurements, therefore, take a shorter time to complete, typically around 1 to 2 hours. As a result, the PSPC measurement is less sensitive to the effects of long term source stability.

Table 1 shows the average effective areas measured for the FM1,2 &3 mirror assemblies with both the PSPC and CCD. These results show that although the CCD errors are larger, the areas derived from both detectors agree to within the experimental errors thus providing an important cross check of the two detector systems.

One further measurement that only the CCD can provide by virtue of its excellent spectral resolving power is an estimate of the position of the gold M edge and the effect that this has on the mirror reflectivity. Figure 9 shows the effective area for the EQM mirror obtained from a continuum source spectrum compared with the theoretical reflectivity values. The main result is that the CCD shows a shift in the edge position of about 30 eV compared to the theory. This shift has also been observed in synchrotron data of reflectivity measurements made on sample gold optical flat[11]. The origin of this effect is attributed to a peak in the density of states for the gold atom which occurs at a higher energy than the absorption edge and dominates the pre-edge structure.

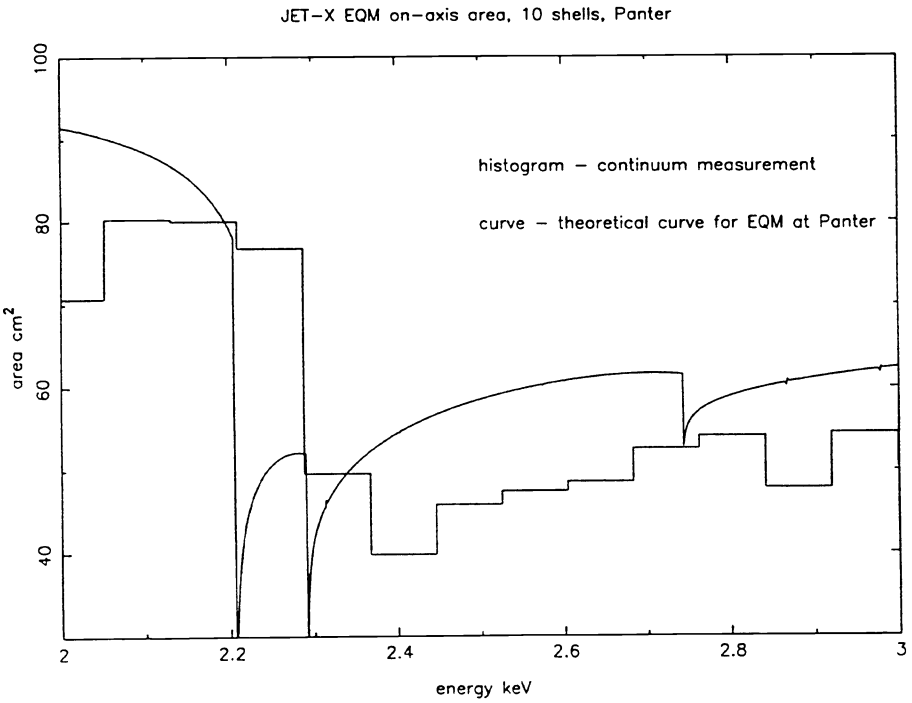

Figure 9 EQM Mirror effective area around the gold M edge obtained using the CCD and a continuum source. Solid line shows the theoretical values.

Energy (keV)	Mirror area (cm2) PSPC	Mirror area (cm2) CCD
1.49	151±2	154±5
8.05	59.1±0.8	54±6

Table 1. Comparison of mirror effective areas at 1.5 & 8keV (average of 2 FM mirrors) obtained with PSPC and CCD detectors.

6.CONCLUSION

The use of the CCD camera for the FM mirror calibration has proved to be an invaluable diagnostic tool. The high spatial resolution and detection efficiency have enabled the mirror imaging performance and the focal length to be measured with precision. Measurement errors of less than 0.1 % for the mirror point spread function and focal length have been achieved. Furthermore, the energy resolution has allowed energy dependent effects to be discriminated.

In comparing the capabilities of the CCD and the PSPC detectors, it is clear that the CCD is much better suited for measurements of mirror focal length and point spread function. The main disadvantage of the CCD camera is its small area, which, for effective area measurements requires long measurement periods and leads to problems arising from source instability. The PSPC requires shorter integration periods and leads to more accurate effective areas. Comparison of the values derived with the two detector systems has, however, enabled an independent cross check to be made and since the two results agree to within the errors, this has given confidence to the estimate of the mirror efficiency measurements derived with the PSPC. An absolute calibration of the mirror area to better than 2%c has been achieved with the PSPC across the X-ray energy band. The PSPC detector is therefore better suited than the CCD for making mirror effective area measurements but a larger area CCD detector would overcome the present limitation.

Following the JET-X mirror calibration, the same CCD camera has been used for preliminary calibrations of the point spread function of the XMM EQM mirrors.

7 ACKNOWLEDGMENTS

The authors acknowledge the help of the Particle Physics and Astronomy Research Council (PPARC) in the UK, The Italian Space Agency (ASI), the Max Plank Institute in Germany and EEV Ltd who manufactured the CCDs used for this project.

8 REFERENCES

1 A. Wells et al, 'JET-X a Joint European X-ray Telescope for Spectrum-X', IAU Coll. No 115, Massachusetts (1988)

2 A. Owens et al, 'The X-ray CCDs developed for the Joint European X-ray Telescope', Journal of X-ray Science & Technology, Accepted for publication May 1996

3 A.D. Holland, M.J.L. Turner, D. Burt and P. Pool, 'The MOS CCDs for the European Photon Imaging Camera', Proc SPIE vol 2006 (1993)

4 B. Aschenbach, H. Brauninger, K.H. Stephen & J. Trumper, 'X-ray test facilities at the Max Plank Institute, Garching', Proc SPIE vol 184, (1979)

5 U. Briel & E. Pfeffernam, 'The position sensitive proportional counter of the ROSAT telescope', Nucl. Inst. & Meth. A242, 376 (1986)

6 G.F. Bignami et al, 'European Photon Imaging Camera for X-ray astronomy', Proc SPIE vol 1344, 132(1990)

7 D. Willingale, 'The Leicester Q analysis software for X-ray data processing',1989

8 O. Citterio et al, 'Optics for the X-ray imaging concentrators aboard the X-ray astronomy satellite SAX', Appl. Opt. 27, 1470(1988)

9 A. Owens et al, 'The effect of XAFS in soft X-ray astronomical telescopes', to appear in Astrophysical Journal 1996